Cell Death and Differentiation (2011) 18, 396–404

www.nature.com/cdd

Cell-autonomous regulation of hematopoietic stem cell cycling activity by ATP

A Casati[1,2,4], M Frascoli[1,4], E Traggiai[3], M Proietti[1], U Schenk[1] and F Grassi*[,1,2]

Extracellular nucleotides regulate many cellular functions through activation of purinergic receptors in the plasma membrane. Here, we show that in hematopoietic stem cell (HSC), ATP is stored in vesicles and released in a calcium-sensitive manner. HSC expresses ATP responsive P2X receptors and *in vitro* pharmacological P2X antagonism restrained hematopoietic progenitors proliferation, but not myeloid differentiation. In mice suffering from chronic inflammation, HSCs were significantly expanded and their cycling activity was sensitive to treatment with the P2X antagonist periodate-oxidized 2,3-dialdehyde ATP. Our results indicate that ATP acts as an autocrine stimulus in regulating HSCs pool size.
Cell Death and Differentiation (2011) **18,** 396–404; doi:10.1038/cdd.2010.107; published online 27 August 2010

Hematopoietic stem cells (HSCs) constitute a minute quiescent and self-renewing cell population with the potential to enter cell cycle and differentiate into progenitors of different cell lineages.[1] Exogenous stimuli can induce HSCs proliferation and differentiation into lineage-committed progenitors. For example, stimulation of toll-like receptors (TLRs) expressed in hematopoietic progenitors was shown to trigger cell cycle entry as well as myeloid differentiation.[2] Interferon-α (IFN-α) was shown to promote exit from G_0 as well as active cell cycling of HSCs, and chronic stimulation of IFN-α receptors led to the exhaustion of stem cell function.[3] Accordingly, interferon regulatory factor-2 (IRF2), a transcriptional suppressor of type I IFN signaling, preserved HSCs self-renewal and differentiation potential.[4] HSCs were also shown to reversibly switch from dormancy to self-renewal upon hematopoietic stress.[5] The definition of factors regulating HSCs self-renewal, expansion and differentiation has important implications not only in hematopoiesis, but also in regenerative medicine and oncology.

Adenosine triphosphate is usually confined inside cells, but after tissue injury and cell death, it can be found in the extracellular space in which it regulates immune cell function as a damage-associated molecular pattern (DAMP). Apart from acting as a DAMP, ATP is constitutively released by various mammalian cell types and concur in setting the basal level of cell activation ('the set point') for signal transduction pathways.[6] In addition, ATP released upon cell activation by a wide range of extracellular stimuli participates in autocrine as well as paracrine feedback loops by binding to purinergic P2 receptors on the cell surface. These receptors are classified into two subgroups termed P2X and P2Y receptors. P2X1–7 receptors bind ATP and open to non-selective cation channels. P2Y1, 2, 4, 6, 11–14 receptors bind ATP, ADP, UDP, UTP or UDP glucose and belong to the family of G-protein-coupled receptors.[7] Extracellular nucleotides were shown to stimulate the proliferation of human HSCs.[8] Herein, we asked whether an autocrine purinergic loop might regulate cell cycling activity of HSCs after stimulation with cytokines or ligands of innate immune system receptors expressed in HSCs. We show that ATP released from an intracellular vesicular compartment positively influences HSC proliferation and regulates the population size of uncommitted hematopoietic progenitors.

Results

Vesicular storage and release of ATP by HSCs. Whereas the intracellular ATP concentration is in the millimolar range, ATP is generally absent in extracellular fluids under physiological conditions. Upon cell death, the high cytosolic ATP content is released and ATP activates P2 receptors in the plasma membrane of surrounding cells, thus transmitting a so-called danger signal. Newer data, however, point also to an important function of ATP as a physiological modulator of several cellular functions.[9] ATP release from healthy cells may occur after a rise in cytosolic calcium, which triggers fusion of ATP-filled vesicles[10] or the opening of pannexin1 hemichannels[11] as well as by membrane stress-induced opening of mechanosensitive channels, such as

[1]Institute for Research in Biomedicine, Bellinzona CH-6500, Switzerland; [2]Dipartimento di Biologia e Genetica per le Scienze Mediche, Universitá degli Studi di Milano, Milano 20133, Italy; [3]Istituto Giannina Gaslini, Genoa 16146, Italy
*Corresponding author: F Grassi, Institute for Research in Biomedicine, Via Vincenzo Vela 6, Bellinzona CH-6500, Switzerland.
Tel: +41 91 820 0323; Fax: +41 91 820 0305; E-mail: fabio.grassi@irb.unisi.ch
[4]These authors contributed equally to this work.
Keywords: hematopoietic stem cell; ATP; cell cycle; purinergic receptors; inflammation
Abbreviations: BM, bone marrow; C/EBP, CCAAT/enhancer-binding protein; CFSE, 5,6-carboxyfluorescein diacetate succinimyl ester; CLP, common lymphoid progenitor; CMP, common myeloid progenitor; DAMP, damage-associated molecular pattern; DKO, double knock-out; FLC, fetal liver chimera; GMP, granulocyte/monocyte progenitor; HSC, hematopoietic stem cell; IBD, inflammatory bowel disease; IFN-α, interferon-α; IL, interleukin; IRF2, interferon regulatory factor-2; LKS, lineage-negative/c-Kit/Sca-1; MEP, megakaryocyte/erythrocyte progenitor; oATP, periodate-oxidized 2′,3′-dialdehyde ATP; RAG, recombinase activating gene; SCF, stem cell factor; TLR, toll-like receptor; TNF, tumor necrosis factor; T_{reg}, T regulatory; v-ATPase, vacuolar H^+ ATPase
Received 05.2.10; revised 14.7.10; accepted 29.7.10; Edited by R De Maria; published online 27.8.10

connexin 43.[12] We determined the subcellular localization of ATP in purified lin$^-$/c-Kit$^+$/Sca-1$^+$ (LKS$^+$) cells, LKS$^+$CD34$^-$ cells, which we refer to as HSCs,[13] and lin$^-$/c-Kit$^+$/Sca-1^{lo} (LKS$^-$) FcγR^{hi}CD34$^+$ granulocyte/monocyte progenitors (GMPs) using the nucleotide-binding fluorescent compound quinacrine. The punctate staining indicative of ATP-filled vesicles detected in HSC (Figure 1A, panel a) and LKS$^+$ cells (not shown) was completely lost after incubation of the cells with bafilomycin A1, a specific inhibitor of vacuolar H$^+$ ATPase, indicating that in hematopoietic progenitor and stem cells, ATP is actively accumulated in vesicles down an electrochemical proton gradient (Figure 1A, panels c and d). In contrast, GMPs did not display a vesicular pattern by quinacrine staining (Figure 1A, panel b). We then verified that ATP-filled secretory granules may be mobilized for exocytosis and mediate ATP release from HSCs after a rise in the cytosolic calcium concentration. LKS$^+$CD34$^-$ cells were stimulated with the calcium ionophore ionomycin and the extracellular ATP was determined by a two-enzyme assay.[14] As shown in Figure 1B, HSCs do release ATP through a calcium-sensitive pathway. Importantly, whereas ATP release was analogously detected in total LKS$^+$ cells (not shown), attempts to detect ATP release by ionomycin in GMPs were unsuccessful (Figure 1B). Calcium imaging experiments of HSCs loaded with the Ca^{2+} indicator Fura-2 revealed the presence of spontaneous calcium oscillations in all cells (Figure 1C). This finding suggests that HSCs may constitutively release quanta (vesicles) of ATP. To investigate whether HSCs were also responsive to extracellular ATP, we analyzed the calcium response of Fura-2 loaded LKS$^+$CD34$^-$ cells stimulated with ATP. Figure 1D shows the prominent increase in cytosolic Ca^{2+} after addition of ATP in all cells. These results suggest that ATP may indeed regulate ATP release from HSCs.[15] Then we asked whether ATP released by hematopoietic progenitor and stem cells might regulate their expansion and differentiation.

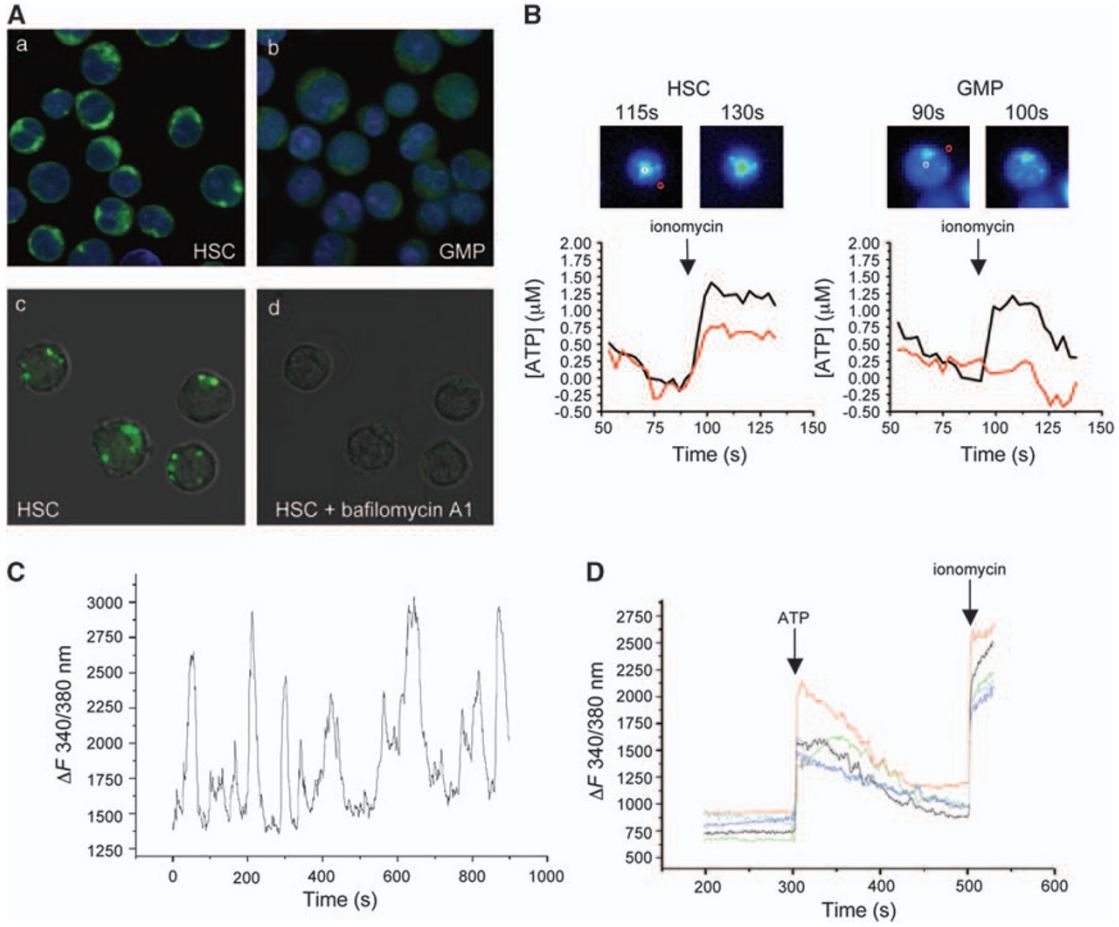

Figure 1 Vesicular storage, release and signaling by ATP in HSCs. (**A**) Sorted LKS$^+$CD34$^-$ HSCs (panel a) and GMPs (panel b) were stained with the nucleotide-binding compound quinacrine as well as nuclear red (DRAQ5), and analyzed in live imaging confocal microscopy. In HSCs, but not GMPs, quinacrine-positive vesicles are visible in the cytoplasm. Quinacrine staining (panel c) was followed by treatment with bafilomycin A1 (panel d). The punctate pattern present in panel c is lost in panel d. (**B**) ATP release from HSC and GMP treated with ionomycin (1 μM) was measured as an increase in NADPH fluorescence generated by a two-enzyme assay. Pseudocolor images and ATP levels in a region of interest (ROI) placed above the cell (black line) or in proximity of the same cell (red line) show the increased fluorescence in the HSC pericellular region. In GMP, the fluorescence increase is limited to the cell body, indicative of calcium-induced mitochondrial NADPH synthesis, but no fluorescence is detected in the pericellular region of the same cell. ATP releasing/monitored cells were 16/24 HSCs and 0/68 GMPs. (**C**) Representative cytosolic Ca^{2+} profile of sorted HSCs loaded with Fura-2. (**D**) Cytosolic Ca^{2+} profiles of sorted HSCs stimulated with ATP (100 μM) and ionomycin (1 μM)

P2X antagonism restrains LKS$^+$ cell proliferation but not myeloid differentiation. Nucleotide-activated P2 receptors were described in human HSCs and exogenous addition of their natural ligands strongly enhanced the stimulatory activity of several cytokines.[8] We assessed P2X receptors expression during HSC differentiation to GMP and LKS$^-$FcγR^{lo}CD34$^-$ megakaryocyte/erythrocyte progenitor (MEP). Figure 2a shows that P2X1, P2X4 and P2X7 are the P2X isoforms expressed in LKS$^+$ cells; all P2X receptors were downregulated upon differentiation to MEP, but not to GMP. TLRs were shown to be expressed in HSCs and to trigger cell cycle entry as well as myeloid differentiation; therefore, they might be important elements in controlling HSCs in inflammatory conditions.[2] Quantitative RT-PCR with TLRs-specific probes revealed the substantial expression of TLR2, 4, 6, 7 and 9 in LKS$^+$ cells and the dramatic downregulation of all TLR transcripts upon transition to MEP (Figure 2b).

P2X-mediated signaling by endogenous ATP was recently shown to significantly contribute to p38 MAPK activation by TLR4 stimulation in microglial cells[16] and to platelet activation by TLR2 stimulation.[17] We, therefore, investigated whether TLR stimulation of LKS$^+$ cells and P2X signaling might synergize in promoting LKS$^+$ cells expansion and differentiation to GMPs. LKS$^+$ cell proliferation in the presence of Flt-3 ligand and stem cell factor (SCF) as well as proliferation induced by stimulation with the TLR2/1 agonist Pam_3CSK_4 or the TLR7/8 agonist R848 were significantly inhibited by periodate-oxidized 2′,3′-dialdehyde ATP (oATP) (Figures 3a and b) in a dose-dependent manner (Supplementary Figure S1). However, the relative frequencies of cycling cells, which progressed to myeloid differentiation, as measured by expression of CD11b, was not influenced by oATP (Figure 3c). In contrast to the inhibition of LKS$^+$ cells expansion, GMPs proliferation in the same conditions was only moderately and non-significantly affected by oATP treatment. Moreover, similar percentages of GMPs acquired F4/80 expression upon TLR stimulation whether oATP was present or not (Supplementary Figure S2). Oxidized ATP was originally described as an irreversible P2X7 antagonist,[18] which was shown to block also other P2X receptor subtypes.[19,20] To address more directly which P2X receptor/s were involved in LKS$^+$ cell proliferation, we used selective pharmacological antagonists for the P2X subtypes expressed in LKS$^+$ cells, namely NF449 for P2X1,[21] 5-BDBD for P2X4 and A-740003 as well as A-438079 for P2X7.[22] LKS$^+$ cell expansion by stimulation with Pam_3CSK_4 or R848 was significantly affected by both NF449 and 5-BDBD, but not by the two P2X7 selective antagonists. The combination of P2X1 and P2X4 antagonists had an additive effect in inhibiting cell expansion, suggesting that both receptors could independently contribute to LKS$^+$ cell cycling activity (Figure 4).

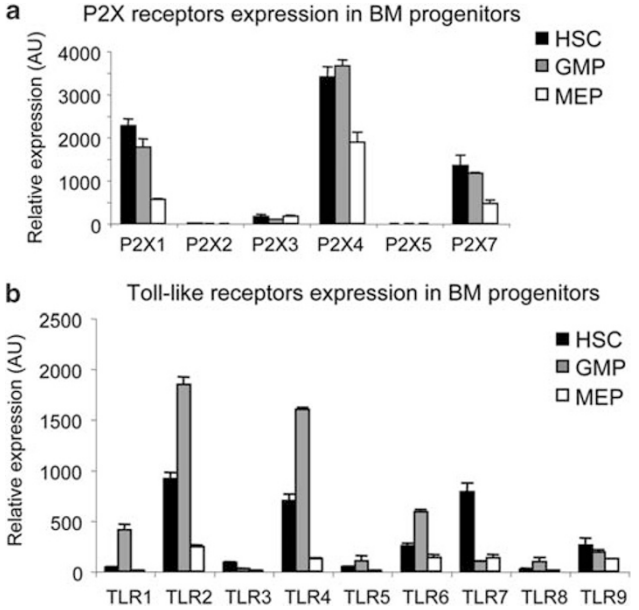

Figure 2 Expression of P2X and toll-like receptors in BM progenitors. Representative experiment showing P2X (**a**) and toll-like (**b**) receptors expression by quantitative real-time PCR on cDNA from the indicated sorted BM cell subsets. Mean values of triplicates ± S.D. from a single experiment representative of two are shown. AU, arbitrary unit

Expansion of HSCs and LKS$^+$ cells during chronic inflammation. To analyze HSCs and hematopoietic progenitors during chronic inflammation, we used calreticulin (crt)-deficient fetal liver chimera (FLC) and mice with inflammatory bowel disease (IBD). *Crt*$^{-/-}$ T cells provoke an inflammatory condition characterized by severe blepharitis and alopecia because of altered regulation of T cell activation.[23] Conversely, adoptive transfer of syngenic naive CD4$^+$ T cell without the immunosuppressive CD25$^+$ T regulatory (T_{reg}) subset into lymphopenic *cd3*$\varepsilon^{-/-}$ mice induces IBD.[24,25] Infections or inflammatory conditions promote granulopoiesis. Immature and mature granulocytes were substantially detected in the spleen and significant increases in CD11b$^+$Gr1^{lo} cells (promyelocytes/myelocytes), CD11b$^+$Gr1^{hi} cells (metamyelocytes/granulocytes)[26] and CD11b^{lo}Gr1^{lo} cells (mainly monocytes) were detected in the bone marrow (BM) of *crt*$^{-/-}$ FLCs and mice with IBD with respect to healthy controls (data not shown). We did not observe significant differences in cell recoveries from the BM in the various experimental groups.

Both *crt*$^{-/-}$ FLCs and mice with IBD displayed non-significantly different LKS$^-$ cell numbers (Figure 5). However, GMPs were significantly increased, whereas MEPs were significantly reduced in the course of inflammation (Figure 6). CCAAT/enhancer-binding protein (C/EBP) α and β are transcription factors involved in common myeloid progenitor to GMP transition and granulopoiesis in response to infections ('emergency' granulopoiesis), respectively.[27] Quantitative analysis of C/EBP α and β transcripts by real-time PCR revealed significantly increased mRNA levels of both transcription factors upon tissue inflammation (data not shown). Enumeration of common lymphoid progenitors (CLPs) as lin$^-$/c-Kit^{lo}/interleukin (IL)-7R$^+$ cells[28] revealed a dramatic depletion of these cells in both *crt*$^{-/-}$ FLCs and mice with IBD (Figure 6). To exclude that the alterations observed in *crt*$^{-/-}$ FLCs were dependent on *crt* deletion in hematopoietic progenitors, we analyzed BM samples from *crt*$^{-/-}$/*cd3*$\varepsilon^{-/-}$ double KO FLCs, which did not display any sign of peripheral tissue inflammation because of the lack of pathogenic T cells;

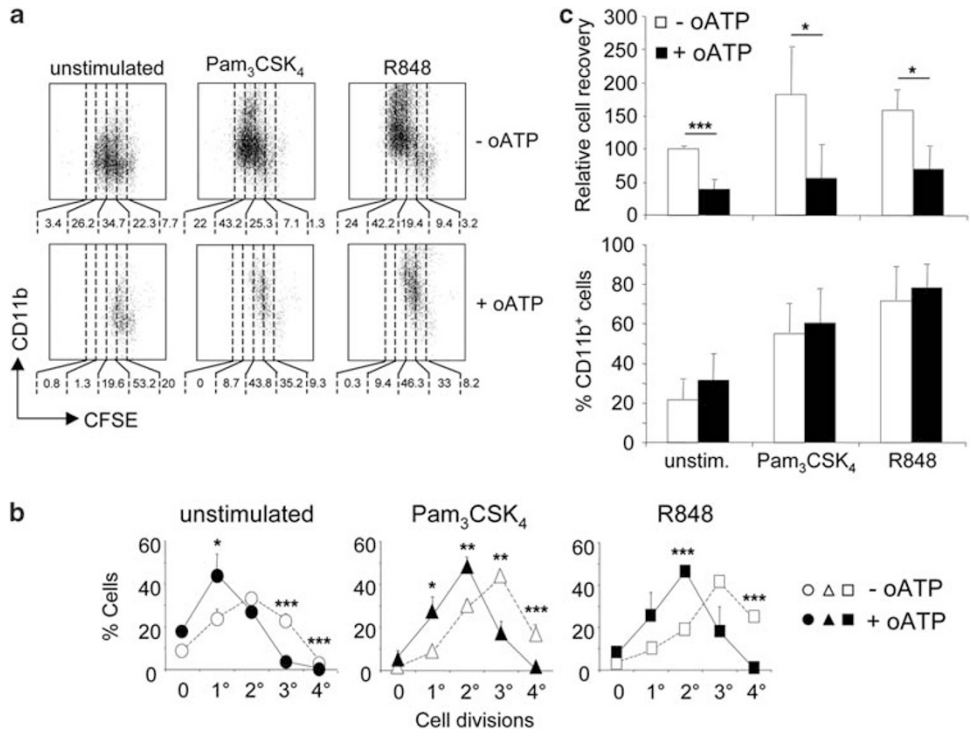

Figure 3 Inhibition of LKS$^+$ cell cycling, but not myeloid differentiation by P2X antagonism. (**a**) Representative CFSE dilution and CD11b staining in purified LKS$^+$ cells cultured in SCF and Flt3L conditioned medium (unstimulated) and with addition of Pam_3CSK_4 (TLR2/1 agonist) or R848 (TLR7/8 agonist) at 1 μg/ml (upper panels). The same experiment performed in the presence of periodate-oxidized 2′,3′-dialdehyde ATP (oATP) at 100 μM is displayed in lower panels. Numbers below the representative dot plots indicate the percentages of cells comprised within the markers. (**b**, **c**) Statistical analysis of three independent experiments with three replicates per point. Mean percentage values ± S.D. ($n = 9$) of cells with the indicated numbers of cell divisions (**b**), mean ± S.D. ($n = 9$) cell recoveries and percentages of CD11b-expressing cells (**c**). $^*P < 0.05$; $^{**}P < 0.01$; $^{***}P < 0.001$

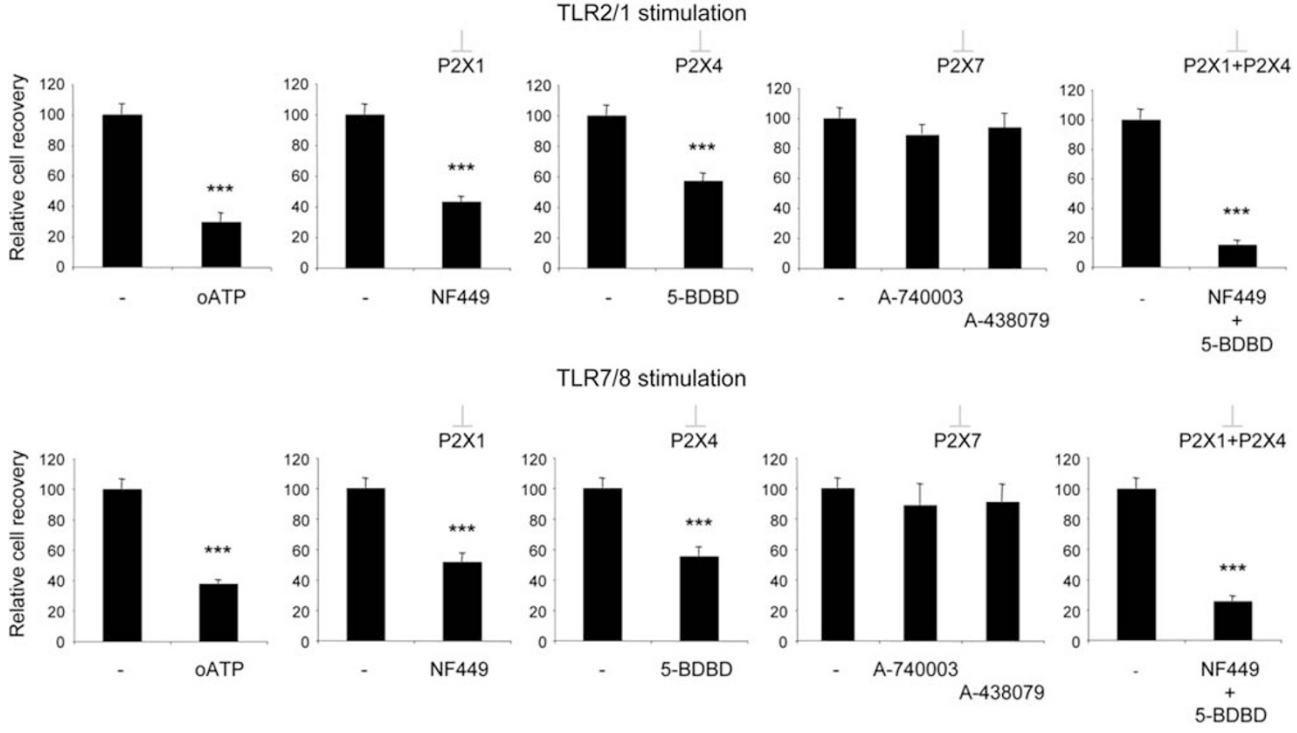

Figure 4 Inhibition of LKS$^+$ cell cycling by selective P2X1 and P2X4 antagonists. Relative recoveries of purified LKS$^+$ cells cultured in SCF and Flt3L conditioned medium in the presence of Pam_3CSK_4 (TLR2/1 agonist) or R848 (TLR7/8 agonist) at 1 μg/ml and the indicated P2X antagonist. Statistical analysis of one representative experiment out of three. Mean ± S.D. cell recoveries of five replicates per point. $^{***}P < 0.001$

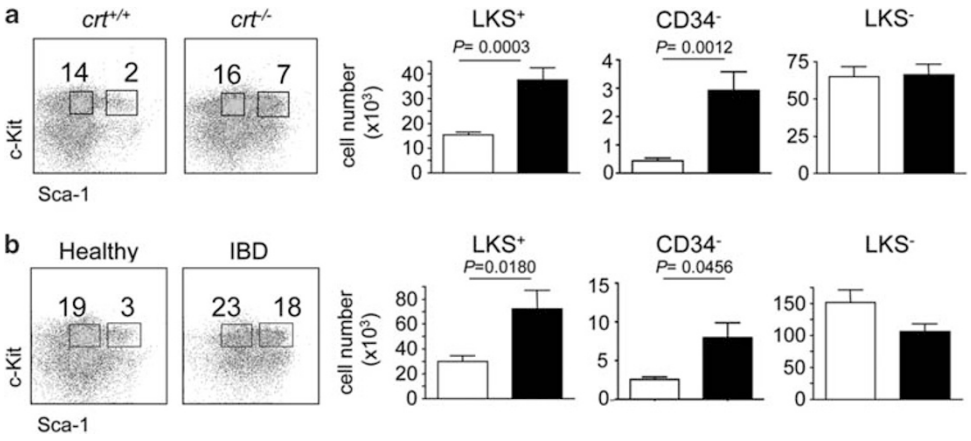

Figure 5 Increased representation of LKS$^+$ cells and HSCs in chronic inflammation. (**a**) Representative dot plot analysis of lin$^-$ BM cells (from femur and tibia) stained with c-Kit and Sca-1 antibodies. Histogram distribution of LKS$^+$, LKS$^+$CD34$^-$ (HSCs) and LKS$^-$ cells absolute numbers (mean ± S.D.) in *crt*$^{+/+}$ (white bars) and *crt*$^{-/-}$ (black bars) FLCs at week 12 from reconstitution ($n=9$). (**b**) Same analysis in healthy controls (white bars) and mice with IBD (black bars) ($n=5$)

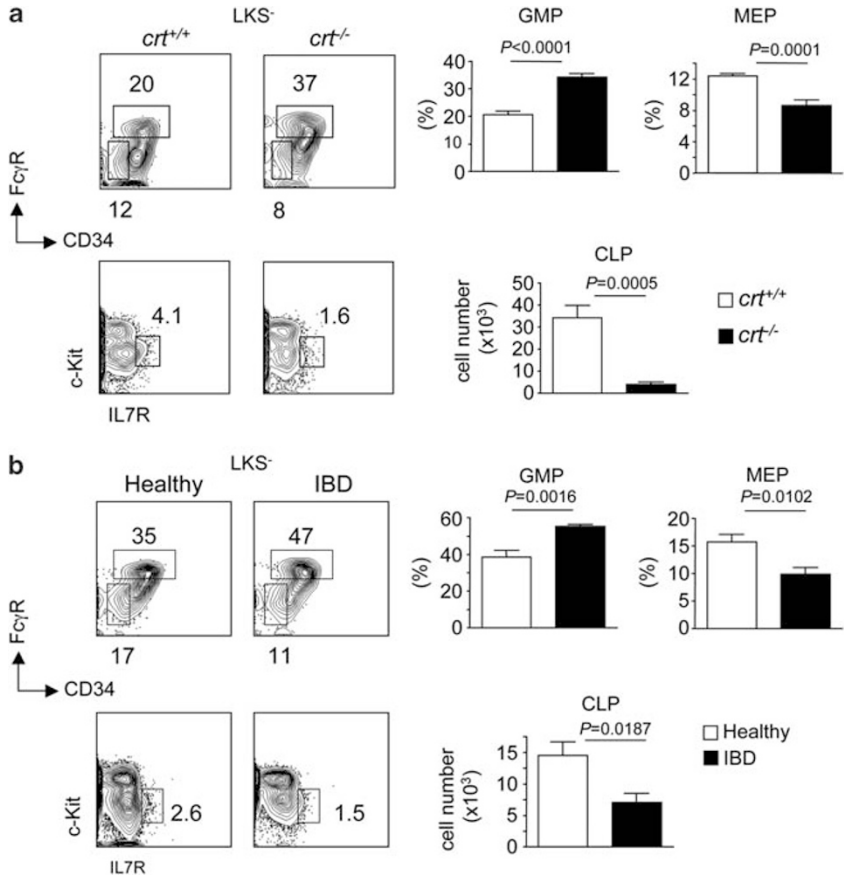

Figure 6 Increased representation of GMPs with reduction of MEPs and CLPs in chronic inflammation. (**a**) Representative dot plot analysis of LKS$^-$ BM cells (from femur and tibia) stained with FcγR and CD34 antibodies, and statistical analysis (mean ± S.D.) of GMPs (FcγR^{hi}CD34$^+$) and MEPs (FcγR^{lo}CD34$^-$) in *crt*$^{+/+}$ (white bars) and *crt*$^{-/-}$ (black bars) FLCs at week 12 from reconstitution (upper panels). Representative dot plot analysis of Lin$^-$ BM cells stained with c-Kit and IL-7R antibodies and histogram distribution (mean ± S.D.) of CLPs (c-Kit^{lo}IL-7R$^+$) expressed as absolute number (lower panels) ($n=9$). (**b**) Same analysis in healthy controls (white bars) and mice with IBD (black bars) ($n=5$)

we could not detect any difference in the representation of the various lineage progenitors in *crt*$^{-/-}$/*cd3ε*$^{-/-}$ with respect to *crt*$^{+/+}$/*cd3ε*$^{-/-}$ FLCs (Supplementary Figure S3).

The results described above document the selective increase of GMPs with depletion of MEPs and CLPs in the course of chronic inflammation.

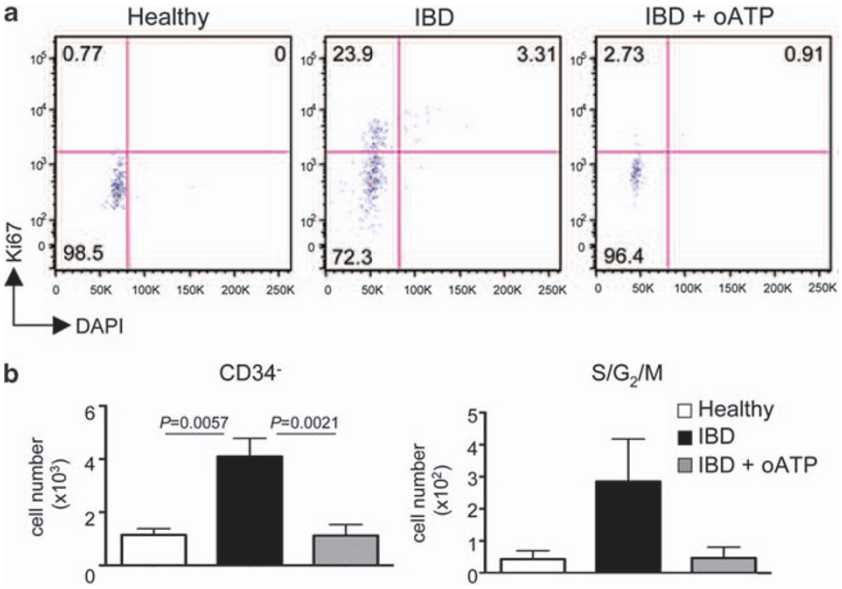

Figure 7 Inhibition of HSCs cycling by P2X antagonism during chronic inflammation. (**a**) Representative dot plot analysis of electronically gated LKS$^+$CD34$^-$ HSCs from bone marrow (femur and tibia from two legs) of healthy controls, mice with IBD and mice with IBD treated with oATP stained with Ki-67 antibody and DAPI. Numbers indicate percentage of cells in the respective quadrant. (**b**) Statistical analysis of HSCs absolute cell numbers (left panel) and HSCs in the S/G_2/M phases of the cell cycle (upper right quadrant in the dot plot analysis above) (right panel) recovered from the different experimental groups (mean ± S.D., $n=5$)

Analysis of LKS$^+$ cells revealed their significant increase in *crt*$^{-/-}$ FLCs (Figure 5a). This increase was not due to *crt* deletion as *crt*$^{-/-}$/*cd3ε*$^{-/-}$ FLCs showed unaltered LKS$^+$ cell representation with respect to *crt*$^{+/+}$/*cd3ε*$^{-/-}$ FLCs (Supplementary Figure S3). To confirm the increased number of LKS$^+$ cells as a feature of chronic inflammation, we performed the same analysis in mice with IBD. As observed in *crt*$^{-/-}$ FLCs, LKS$^+$ cells were significantly increased during IBD (Figure 5b). We observed some differences in absolute cell numbers of progenitors between the various experimental groups, which were likely due to the different genetic backgrounds. As acute exposure to TNF-α and IL-6 was shown to induce phenotypic inversion of LKS$^-$ to LKS$^+$ cells by upregulation of Sca-1,[29] we checked whether chronic tissue inflammation determined Sca-1 expression by lineage-committed progenitors. To this end, we analyzed LKS$^+$ cells for expression of FcγRII/III and IL-7Rα chain, which are not expressed by bona fide uncommitted LKS$^+$ cells. LKS$^+$ cells from all groups of mice were phenotypically indistinguishable and neither expressed FcγRII/III nor IL-7Rα (data not shown), ruling out phenotypic inversion of LKS$^-$ cells in chronic inflammation.

Inhibition of HSC cycling activity by P2X antagonism during chronic inflammation. To check whether chronic inflammation affected HSC quiescence, we investigated the representation of HSCs in the different experimental groups. This analysis revealed the robust increase of this cell subset in both *crt*$^{-/-}$ FLCs and mice with IBD compared with the healthy counterparts (Figure 5), thus suggesting that chronic inflammation determines entry into the cell cycle and expansion of the quiescent self-renewing pool of HSCs. To see whether P2X activation contributed to HSCs expansion *in vivo*, we treated mice suffering from IBD with oATP for 5 days and then scored hematopoietic progenitors in the BM. Notably, LKS$^+$ cells (Supplementary Figure S4) and HSCs (Figure 7b) were significantly reduced by oATP treatment. Analysis of cell cycling activity by staining with Ki-67 mab and DAPI revealed the substantial decrease of cells in S/G_2/M phases of the cell cycle upon treatment with oATP (Figure7; Supplementary Figure S4). These results indicate that P2X activation crucially contributes to HSCs expansion during inflammation, thus pointing to a function for extracellular ATP as a regulator of HSCs population size.

Discussion

HSC activity is concentrated in few cells, which in mice enter a quiescent state few weeks after birth.[30] A hibernation system similar to *Caenorhabditis elegans* dauer formation is used by HSC to lower cell metabolism and modulate cytokine signaling.[31] Dormancy of HSCs is instrumental in maintaining the blood repopulating potential of the BM for a lifetime. Indeed, chronic HSCs cycling leads to loss of stemness and exhaustion of the hematopoietic potential, which might be fatal for the organism.[3] Furthermore, as tumors may often originate from the transformation of normal stem cells, stem cells quiescence appears important to protect the organism from cancer.[32] Interactions with other cells, soluble factors and extracellular matrix composing HSCs niches in the BM contribute to setting HSCs dormancy, self-renewal and/or expansion.[33–35] In two murine models of T cell-mediated chronic inflammation, namely *crt*$^{-/-}$ FLC[23] and IBD,[24,25] we found that HSCs and LKS$^+$ cells were expanded together with increased granulopoiesis and significant reductions of both MEPs and CLPs. We have shown that *in vitro* and *in vivo* during chronic inflammation extracellular ATP contributes to HSCs and LKS$^+$ cells expansion.

Innate immune response receptors were shown to be expressed in HSCs and to regulate their proliferation and myeloid differentiation.[2,3,5] Extracellular ATP significantly increased cell cycling activity of purified LKS$^+$ cells *in vitro*; however, the frequency of myeloid differentiation of TLR-activated LKS$^+$ cells entering the cell cycle as well as cycling of purified GMPs were not affected by the P2X antagonist oATP. Notably, we were unable to detect ATP release from GMPs after increase in cytosolic calcium. These results indicate that extracellular ATP regulates HSCs cycling activity in a cell-autonomous manner.

Quinacrine staining of HSCs showed that ATP is stored in a vesicular compartment. P2X1, 4 and 7 are the predominant P2X isoforms expressed in murine hematopoietic stem and progenitors cells and are all downregulated upon transition to MEP. These receptors were functional in HSCs as addition of exogenous ATP determined a prominent Ca^{2+} influx. Using selective pharmacological antagonists, we showed that P2X1 and P2X4 are the two P2X receptor subtypes, which contribute purinergic feedback loops in LKS$^+$ cell proliferation. Moreover, pharmacological P2X antagonism inhibited HSCs expansion during chronic inflammation. Therefore, an increase of extracellular ATP in the hematopoietic niche might lead to sustained release of ATP by HSCs through ATP-mediated calcium influx and triggering of vesicle fusion. In the vascular system, when ATP reaches a critical extracellular concentration, it stimulates the release of ATP by endothelial cells and this self-perpetuating release was suggested to have an important function in vascular control.[15] An analogous self-perpetuating release of ATP by HSCs might have an important function in controlling the cycling activity of HSCs in physiological and pathological conditions. Notably, endothelial progenitors and HSCs both originate from hemangioblasts in embryonic life and share several survival as well as chemotactic signaling pathways in adulthood.[36]

Both trabecular osteoblasts[34,37] and sinusoidal endothelium[38] constitute functional niches, which support HSCs in the BM. Several observations point to a function of the osteoblastic niche in determining HSC quiescence: (i) increase of N-cadherin$^+$ osteoblasts, an important component of the niche, resulted in parallel increase of non-cycling HSCs;[37] (ii) osteoblasts deficiency resulted in depletion of HSCs in the BM;[39] (iii) Tie2/angiopoietin-1 signaling in the osteoblastic niche was shown to regulate HSCs quiescence.[33] Conversely, other evidences suggest that the vascular niche is poised to differentiation of hematopoietic progenitors[40,41] and it was hypothesized that the vascular niche would support proliferation and mobilization of activated HSCs.[42] Endothelial cells are a source of extracellular ATP under conditions of hypoxia, increased shear stress and chemical or mechanical stimulation.[43–45] A sustained ATP release by endothelial cells might preferentially shift HSCs from quiescence to expansion in perivascular niches. Interestingly, fluid shear stress increases hematopoietic colony-forming potential and expression of hematopoietic markers in the aorta–gonads–mesonephros region of mouse embryos.[46] Signaling by this biomechanical force was mediated by nitric oxide; it is tempting to speculate that ATP release by endothelial cells and purinergic signaling in HSCs might contribute to implement HSCs expansion also at this early developmental stage. Finally, the results presented here points to both a putative action of ATP on HSCs homeostasis and to an intrinsic function of endogenous ATP in regulating the cycling activity of the HSC.

Materials and Methods

Mice. *Crt*$^{+/-}$ (H-2^b) mice,[23] BALB/c recombinase activating gene (RAG)/γ chain double knock-out (DKO) (H-2^d) mice obtained from Dr. Mamoru Ito (Central Institute for Experimental Animals, Miyamae, Kawasaki, Japan) and *cd3e*$^{-/-}$ mice from Jackson Laboratory (Bar Harbor, ME, USA) were bred and treated in accordance with the Swiss Federal Veterinary Office guidelines. Experiments were approved by 'Dipartimento della Sanità e della Socialità'. FLCs in RAG/γ chain DKO mice with *crt*$^{+/+}$ and *crt*$^{-/-}$ progenitors were generated as described.[23] Briefly, sublethally irradiated mice were intravenously injected with 2×10^6 genotyped fetal liver cells in 200 μl PBS. Analogously, FLCs with *crt*$^{-/-}$/*cd3e*$^{-/-}$ and *crt*$^{+/+}$/*cd3e*$^{-/-}$ progenitors were generated by breeding *crt*$^{+/-}$/*cd3e*$^{-/-}$ mice. For treatment with oATP, mice were injected in the tail vein with 100 μl of 3 mM oATP (Sigma-Aldrich, Buchs, Switzerland) in PBS once a day.

Flow cytometry. For FACS analysis, mAbs conjugated with either biotin, FITC, PE, CyChrome, PerCP, Alexa588, PE-Cy5, Pe-Cy7, APC-Cy7 or APC against the following antigens were used: CD8a (53-6.7), CD62L (MEL-14), CD25 (PC61.5), CD4 (L3T4), Gr-1 (RB6-8C5), CD2 (RM2-5), CD44 (IM7), CD19 (6D5), CD11b (M1/70), CD34 (RAM34), IL-7R (A7R34), FcγR/CD16/35 (2.4G2), c-Kit/CD117 (ACK2), F4/80 (BM8), Ter119 (TER-199), CD11c (N418), (eBioscence, San Diego, CA, USA); CD45R/B220 (RA3-6B2), IgM (II/41), IgD (11.26c.2a), Sca-1 (E13-161.7), NK1.1 (PK136), Ki-67 (B56) and APC-Cy7-streptavidin (BD Bioscience, Allschwil, Switzerland). For cell cycle analysis with Ki-67 mAb, cells were stained with PerCP-conjugated Lin-specific mAbs, PE-Cy7-conjugated Sca-1, APC-conjugated CD34 and APC-Cy7 CD117 mAbs. Then, cells were fixed and permeabilized with 'Fix and Perm' (BD Bioscience) followed by staining with FITC-conjugated Ki-67 or control anti-IgG$_1$ mAb and DAPI at 1 μg/ml. All samples were acquired with a FACSCalibur or FACSCanto (Becton Dickinson, Allschwil, Switzerland) and analyzed with FlowJo software (Treestar Inc., Ashland, OR, USA). Statistical analysis was performed by using a Student's *t*-test. Data are reported as mean $\pm$ S.D. Values of $P < 0.05$ were considered significant. For cell sorting, labeled cells were sorted with FACSAria (Becton Dickinson).

Induction of IBD. For IBD induction, T cells were isolated from peripheral lymph nodes and spleen of C57BL/6 mice by positive selection with anti-CD4-coated immunomagnetic beads (Miltenyi Biotech, Bergisch Gladbach, Germany) followed by cells sorting. CD4$^+$ naive (CD4$^+$CD44$^-$CD25$^-$CD62L$^+$) and regulatory (CD4$^+$CD25$^+$) T cell subsets were sorted at FACSAria (Becton Dickinson). *Cd3e*$^{-/-}$ mice were intravenously injected with 0.4×10^6 CD4$^+$ naive T cells. As a control, mice were injected with CD4 naive cells together with 0.2×10^6 CD4$^+$CD25$^+$ T_{reg} cells. Mice were weighted weekly and were killed at week 5 after cell transfer, when IBD was diagnosed by severe diarrhea and weight loss. For cell cycle analysis of HSCs, mice were analyzed at week 3 after IBD induction.

Quantification of mRNA levels. Total RNA was precipitated in Trizol (Invitrogen, Basel, Switzerland) and then reverse transcribed to cDNA using Random hexamer primers and an M-MLV reverse-transcriptase kit (Invitrogen). For quantification of transcripts, mRNA samples were treated with 2 U/sample of DNase (Applied Biosystems, Zug, Switzerland). Transcripts were quantified by real-time quantitative PCR on an ABI PRISM 7700 Sequence Detector with predesigned TaqMan Gene Expression Assays and reagents according to the manufacturer's instructions (PerkinElmer Applied Biosystems, Schwerzenbach, Switzerland). Probes with the following Applied Biosystems assay identification numbers were used:

TLR1	Mm00446095_m1
TLR2	Mm00442346_m1
TLR3	Mm00446577_g1
TLR4	Mm00445274_m1
TLR5	Mm00546288_s1
TLR6	Mm02529782_m1
TLR7	Mm00446590_m1
TLR8	Mm01157262_m1
TLR9	Mm00446193_m1

P2X1	Mm00435460_m1
P2X2	Mm01202369_g1
P2X3	Mm00523699_m1
P2X4	Mm00501787_m1
P2X5	Mm00473677_m1
P2X7	Mm00440582_m1
18S	EUK 18S rRNA (DQ) Mix

For each sample, mRNA abundance was normalized to the amount of 18S rRNA and is presented in arbitrary units.

Analysis of cell proliferation. Sorted GMPs and LKS^+ cells were labeled with 5,6-carboxyfluorescein diacetate succinimyl ester (CFSE) (Molecular Probes, Basel, Switzerland), seeded in αMEM medium with 2% FCS (Hyclone, Lausanne, Switzerland), 50 μM β-mercaptoethanol, 1% penicillin/streptomycin, 20 ng/ml SCF, 100 ng/ml Flt3L and stimulated with Pam_3CSK_4 or R848 (InvivoGen, San Diego, CA, USA) at 1 μg/ml. Where indicated, oATP was added at a final concentration of 100 μM and left in culture for the 72-h period of the assay. As measured by flow cytometry, each division of CFSE-labeled cells causes a twofold reduction in mean fluorescent intensity (MFI) in the daughter cell, with the result that extensive cell proliferation results in a progressive step-wise reduction in MFI. To quantify cell recoveries, FACS acquisitions were standardized by fixed numbers of calibration beads (BD Pharmingen, Allschwil, Switzerland). For selective antagonism of P2 receptors, 30 μM NF449 for P2X1, 100 μM 5-BDBD for P2X4, 10 μM A-740003 or 10 μM A-438079 for P2X7 (all from Tocris Bioscience, Bristol, UK) were used. Statistical analysis was performed by using a Student's *t*-test. Values of $P < 0.05$ were considered significant.

Microscopy, calcium imaging and analysis of ATP release. Laser scanning confocal microscopy was performed with a Leica DI6000 microscope stand connected to a SP5 scan head equipped with a temperature-controlled chamber. Live cell cultures were placed in a humidified and CO_2-controlled incubator, which was mounted on the microscope stage. Purified HSCs, GMPs or LKS^+ cells were rested after cell sorting in αMEM medium with SCF and Flt3L for 16 h, then stained with 0.5 μM quinacrine for 30 min at 37°C; where indicated 5 μM bafilomycin A1 was added. Nuclear red (DRAQ5) was used to distinguish nuclei in live imaging.

For calcium imaging, cells were loaded for 20 min at room temperature with 5 μM Fura-2 pentacetoxy methylester and plated on poly-L-lysine-coated coverslips. Coverslips were then washed and transferred to the recording chamber of an inverted microscope (Axiovert 200, Zeiss, Feldbach, Switzerland) equipped with Andor 885 JCS iXON classic camera. For Ca^{2+} measurements, Polychrome V (Till Photonics, Gräfelfing, Germany) was used as a light source. After excitation at 340 and 380 nm wavelengths, the emitted light was acquired at 505 nm. The sampling rate was 1 Hz. Ca^{2+} concentrations were expressed as 340/380 fluorescence ratio. The ratio values in discrete areas of interest were calculated with TILLvisION software from sequences of images in order to obtain temporal analyses. The experiments were performed in modified Krebs–Ringer solution (KRH): 155 mM NaCl, 4.5 mM KCl, 10 mM glucose, 5 mM HEPES pH 7.4, 1 mM $MgCl_2$, 2 mM $CaCl_2$ at 28–30°C.

ATP release was measured by means of a two-enzyme assay, as described.[14] Briefly, cells were plated on polylysine-coated coverslips, which were fixed in the recording chamber of an inverted microscope. Cells were incubated in KRH supplemented with 8 U/ml each of hexokinase and glucose 6-phosphate dehydrogenase and 5 mM NADP. In the presence of ATP, these enzymes catalyze the formation of NADPH, a fluorescent molecule that was visualized using fluorescence microscopy with an excitation wavelength of 340 nm and an emission at 460 nm. The fluorescence intensity of regions on or outside the cells was measured using TILLvisION software and ATP concentrations were estimated using ATP standard solutions of known concentrations. The solution used for this assay shows low levels of autofluorescence, which bleaches over time after illumination. For this reason, a steady decrease of the baseline signal is observed in the course of the experiment. In the plots shown in Figure 1, background levels of fluorescence were subtracted at time of ionomycin addition, which might lead to negative values in the absence of ATP release.

Conflict of interest

The authors declare no conflict of interest.

Acknowledgements. We thank Enrica Mira Catò, Luana Perlini (IRB, Bellinzona, Switzerland) for technical assistance; David Jarrossay (IRB, Bellinzona, Switzerland) for expert support at FACS and cell sorting; Nobuyuki Onai, Hitoshi Takizawa and Markus Manz for precious advice (Institute for Research in Biomedicine, Bellinzona, Switzerland) and Mamoru Ito (Laboratory of Immunology, CIEA, Kawasaki, Japan) for providing RAG/γ chain DKO mice. This work was supported by grants to FG from Swiss National Science Foundation, Fondazione Ticinese per la Ricerca sul Cancro, Fondazione per la Ricerca sulla Trasfusione e sui Trapianti, European School of Oncology Foundation, G.G.G. Foundation and the Sixth Research Framework Programme of the European Union, Project MUGEN (MUGEN LSHB-CT-2005-005203). AC is a recipient of a fellowship from Fondazione Stella Major and MF is a recipient of a fellowship from Swiss Cancer League/Oncosuisse.

1. Weissman IL. Stem cells: units of development, units of regeneration, and units in evolution. *Cell* 2000; **100**: 157–168.
2. Nagai Y, Garrett KP, Ohta S, Bahrun U, Kouro T, Akira S *et al.* Toll-like receptors on hematopoietic progenitor cells stimulate innate immune system replenishment. *Immunity* 2006; **24**: 801–812.
3. Essers MA, Offner S, Blanco-Bose WE, Waibler Z, Kalinke U, Duchosal MA *et al.* IFNalpha activates dormant haematopoietic stem cells *in vivo*. *Nature* 2009; **458**: 904–908.
4. Sato T, Onai N, Yoshihara H, Arai F, Suda T, Ohteki T. Interferon regulatory factor-2 protects quiescent hematopoietic stem cells from type I interferon-dependent exhaustion. *Nat Med* 2009; **15**: 696–700.
5. Wilson A, Laurenti E, Oser G, van der Wath RC, Blanco-Bose W, Jaworski M *et al.* Hematopoietic stem cells reversibly switch from dormancy to self-renewal during homeostasis and repair. *Cell* 2008; **135**: 1118–1129.
6. Corriden R, Insel PA. Basal release of ATP: an autocrine-paracrine mechanism for cell regulation. *Sci Signal* 2010; **3**: re1.
7. Burnstock G. Purinergic signaling – an overview. *Novartis Found Symp* 2006; **276**: 26–48; discussion 48–57, 275–281.
8. Lemoli RM, Ferrari D, Fogli M, Rossi L, Pizzirani C, Forchap S *et al.* Extracellular nucleotides are potent stimulators of human hematopoietic stem cells *in vitro* and *in vivo*. *Blood* 2004; **104**: 1662–1670.
9. Surprenant A, North RA. Signaling at purinergic P2X receptors. *Annu Rev Physiol* 2008; **71**: 333–359.
10. Coco S, Calegari F, Pravettoni E, Pozzi D, Taverna E, Rosa P *et al.* Storage and release of ATP from astrocytes in culture. *J Biol Chem* 2003; **278**: 1354–1362.
11. Locovei S, Bao L, Dahl G. Pannexin 1 in erythrocytes: function without a gap. *Proc Natl Acad Sci USA* 2006; **103**: 7655–7659.
12. Kang J, Kang N, Lovatt D, Torres A, Zhao Z, Lin J *et al.* Connexin 43 hemichannels are permeable to ATP. *J Neurosci* 2008; **28**: 4702–4711.
13. Osawa M, Hanada K, Hamada H, Nakauchi H. Long-term lymphohematopoietic reconstitution by a single CD34-low/negative hematopoietic stem cell. *Science* 1996; **273**: 242–245.
14. Corriden R, Insel PA, Junger WG. A novel method using fluorescence microscopy for real-time assessment of ATP release from individual cells. *Am J Physiol Cell Physiol* 2007; **293**: C1420–C1425.
15. Bodin P, Burnstock G. ATP-stimulated release of ATP by human endothelial cells. *J Cardiovasc Pharmacol* 1996; **27**: 872–875.
16. Clark AK, Staniland AA, Marchand F, Kaan TK, McMahon SB, Malcangio M. P2X7-dependent release of interleukin-1beta and nociception in the spinal cord following lipopolysaccharide. *J Neurosci* 2010; **30**: 573–582.
17. Kalvegren H, Skoglund C, Helldahl C, Lerm M, Grenegard M, Bengtsson T. Toll-like receptor 2 stimulation of platelets is mediated by purinergic P2X1-dependent Ca2+ mobilisation, cyclooxygenase and purinergic P2Y1 and P2Y12 receptor activation. *Thromb Haemost* 2010; **103**: 398–407.
18. Murgia M, Hanau S, Pizzo P, Rippa M, Di Virgilio F. Oxidized ATP. An irreversible inhibitor of the macrophage purinergic P2Z receptor. *J Biol Chem* 1993; **268**: 8199–8203.
19. Evans RJ, Lewis C, Buell G, Valera S, North RA, Surprenant A. Pharmacological characterization of heterologously expressed ATP-gated cation channels (P2x purinoceptors). *Mol Pharmacol* 1995; **48**: 178–183.
20. Jacques-Silva MC, Correa-Medina M, Cabrera O, Rodriguez-Diaz R, Makeeva N, Fachado A *et al.* ATP-gated P2X3 receptors constitute a positive autocrine signal for insulin release in the human pancreatic beta cell. *Proc Natl Acad Sci USA* 2010; **107**: 6465–6470.
21. Rettinger J, Braun K, Hochmann H, Kassack MU, Ullmann H, Nickel P *et al.* Profiling at recombinant homomeric and heteromeric rat P2X receptors identifies the suramin analogue NF449 as a highly potent P2X1 receptor antagonist. *Neuropharmacology* 2005; **48**: 461–468.
22. Donnelly-Roberts D, McGaraughty S, Shieh CC, Honore P, Jarvis MF. Painful purinergic receptors. *J Pharmacol Exp Ther* 2008; **324**: 409–415.
23. Porcellini S, Traggiai E, Schenk U, Ferrera D, Matteoli M, Lanzavecchia A *et al.* Regulation of peripheral T cell activation by calreticulin. *J Exp Med* 2006; **203**: 461–471.
24. Bouma G, Strober W. The immunological and genetic basis of inflammatory bowel disease. *Nat Rev Immunol* 2003; **3**: 521–533.

25. Mottet C, Uhlig HH, Powrie F. Cutting edge: cure of colitis by CD4+CD25+ regulatory T cells. *J Immunol* 2003; **170**: 3939–3943.
26. Ueda Y, Kondo M, Kelsoe G. Inflammation and the reciprocal production of granulocytes and lymphocytes in bone marrow. *J Exp Med* 2005; **201**: 1771–1780.
27. Hirai H, Zhang P, Dayaram T, Hetherington CJ, Mizuno S, Imanishi J *et al.* C/EBPbeta is required for 'emergency' granulopoiesis. *Nat Immunol* 2006; **7**: 732–739.
28. Kondo M, Weissman IL, Akashi K. Identification of clonogenic common lymphoid progenitors in mouse bone marrow. *Cell* 1997; **91**: 661–672.
29. Zhang P, Nelson S, Bagby GJ, Siggins II R, Shellito JE, Welsh DA. The lineage-c-Kit+Sca-1+ cell response to Escherichia coli bacteremia in Balb/c mice. *Stem Cells* 2008; **26**: 1778–1786.
30. Bowie MB, McKnight KD, Kent DG, McCaffrey L, Hoodless PA, Eaves CJ. Hematopoietic stem cells proliferate until after birth and show a reversible phase-specific engraftment defect. *J Clin Invest* 2006; **116**: 2808–2816.
31. Yamazaki S, Iwama A, Takayanagi S, Morita Y, Eto K, Ema H *et al.* Cytokine signals modulated via lipid rafts mimic niche signals and induce hibernation in hematopoietic stem cells. *EMBO J* 2006; **25**: 3515–3523.
32. Reya T, Morrison SJ, Clarke MF, Weissman IL. Stem cells, cancer, and cancer stem cells. *Nature* 2001; **414**: 105–111.
33. Arai F, Hirao A, Ohmura M, Sato H, Matsuoka S, Takubo K *et al.* Tie2/angiopoietin-1 signaling regulates hematopoietic stem cell quiescence in the bone marrow niche. *Cell* 2004; **118**: 149–161.
34. Calvi LM, Adams GB, Weibrecht KW, Weber JM, Olson DP, Knight MC *et al.* Osteoblastic cells regulate the haematopoietic stem cell niche. *Nature* 2003; **425**: 841–846.
35. Yamazaki S, Iwama A, Takayanagi S, Eto K, Ema H, Nakauchi H. TGF-beta as a candidate bone marrow niche signal to induce hematopoietic stem cell hibernation. *Blood* 2009; **113**: 1250–1256.
36. Hattori K, Dias S, Heissig B, Hackett NR, Lyden D, Tateno M *et al.* Vascular endothelial growth factor and angiopoietin-1 stimulate postnatal hematopoiesis by recruitment of vasculogenic and hematopoietic stem cells. *J Exp Med* 2001; **193**: 1005–1014.
37. Zhang J, Niu C, Ye L, Huang H, He X, Tong WG *et al.* Identification of the haematopoietic stem cell niche and control of the niche size. *Nature* 2003; **425**: 836–841.
38. Kiel MJ, Yilmaz OH, Iwashita T, Terhorst C, Morrison SJ. SLAM family receptors distinguish hematopoietic stem and progenitor cells and reveal endothelial niches for stem cells. *Cell* 2005; **121**: 1109–1121.
39. Visnjic D, Kalajzic Z, Rowe DW, Katavic V, Lorenzo J, Aguila HL. Hematopoiesis is severely altered in mice with an induced osteoblast deficiency. *Blood* 2004; **103**: 3258–3264.
40. Avecilla ST, Hattori K, Heissig B, Tejada R, Liao F, Shido K *et al.* Chemokine-mediated interaction of hematopoietic progenitors with the bone marrow vascular niche is required for thrombopoiesis. *Nat Med* 2004; **10**: 64–71.
41. Kopp HG, Avecilla ST, Hooper AT, Rafii S. The bone marrow vascular niche: home of HSC differentiation and mobilization. *Physiology (Bethesda)* 2005; **20**: 349–356.
42. Arai F, Suda T. Maintenance of quiescent hematopoietic stem cells in the osteoblastic niche. *Ann N Y Acad Sci* 2007; **1106**: 41–53.
43. Bodin P, Bailey D, Burnstock G. Increased flow-induced ATP release from isolated vascular endothelial cells but not smooth muscle cells. *Br J Pharmacol* 1991; **103**: 1203–1205.
44. Gerasimovskaya EV, Ahmad S, White CW, Jones PL, Carpenter TC, Stenmark KR. Extracellular ATP is an autocrine/paracrine regulator of hypoxia-induced adventitial fibroblast growth. Signaling through extracellular signal-regulated kinase-1/2 and the Egr-1 transcription factor. *J Biol Chem* 2002; **277**: 44638–44650.
45. Sedaa KO, Bjur RA, Shinozuka K, Westfall DP. Nerve and drug-induced release of adenine nucleosides and nucleotides from rabbit aorta. *J Pharmacol Exp Ther* 1990; **252**: 1060–1067.
46. Adamo L, Naveiras O, Wenzel PL, McKinney-Freeman S, Mack PJ, Gracia-Sancho J *et al.* Biomechanical forces promote embryonic haematopoiesis. *Nature* 2009; **459**: 1131–1135.

Supplementary Information accompanies the paper on Cell Death and Differentiation website (http://www.nature.com/cdd)